Cross-sectional transmission electron microscopy study of 1.5 MeV Kr^+ irradiation-induced amorphization in α-quartz

W. L. Gong[a)]
Department of Earth and Planetary Sciences, University of New Mexico, Albuquerque, New Mexico 87131

L. M. Wang and R. C. Ewing
Department of Nuclear Engineering and Radiological Sciences, The University of Michigan, Ann Arbor, Michigan 48109

(Received 20 March 1998; accepted for publication 22 July 1998)

Cross-sectional and high-resolution transmission electron microscopy (XTEM and HRTEM, respectively) have been used to characterize ion-beam-induced amorphization of α-quartz irradiated with 1.5 MeV Kr^+ ions at room temperature. The accumulation of damage and the growth of the amorphous layers in quartz were studied as a function of ion fluence up to 1.7×10^{14} ions/cm^2. An amorphous band was first observed at the peak displacement damage range, and this region increased in width with increasing ion fluence. These results demonstrate that direct displacement damage by nuclear collision is more efficient than ionization processes in inducing amorphization in quartz. At lower fluences ($\leqslant 1.7\times10^{13}$ ions/cm^2), the damage profile observed by XTEM is in excellent agreement with the distribution of displacement damage predicted by TRIM calculations. At higher fluences, the range of the amorphous band measured by XTEM exceeds the depth predicted by TRIM. © *1998 American Institute of Physics.* [S0021-8979(98)09920-4]

I. INTRODUCTION

Silica in its crystalline and amorphous forms has a wide spectrum of industrial applications in integrated optics and microelectronic technology.[1,2] For example, α-quartz has been used for fabrication of optical waveguides[3] and piezoelectric devices.[4] A fundamental requirement for optical waveguides in transparent materials is to define a region of high refractive index within a lower index material. Ion beam techniques have been applied to directly create the waveguide region by implanting chemical dopants to change the refractive index or by ion-beam-induced damage which lower the refractive index.[5,6] The refractive index profile of a quartz waveguide has been studied as a function of He^+ ion fluence.[7] Implantation of metallic ions such as Ti^+, Cu^+, Ga^+, and Ag^+ into quartz substrates has been previously performed in order to form a conductive surface layer to resolve problems with packaging and hermetic sealing of a microsensor device.[4,8] In this previous work, Rutherford backscattering spectroscopy channeling experiments (RBS-C) were extensively used to provide depth profiles of the implanted ions and radiation-induced damage zone, and these profiles were then compared to simulations from TRIM code calculations.

Amorphization can be induced by radiolysis or ionization in electron and light-ion irradiated quartz.[9–11] Amorphization can also be induced by displacement cascade processes by the heavy ion irradiation of quartz.[12,13] For the energetic charged particles, energy loss is mainly through both ionization and elastic collision processes. The two types of energy loss of energetic ions in solids are both depth dependent, as is the damage distribution.[14] By comparing the energy loss profile with the actual damage distribution, the mechanism mainly responsible for the damage may be understood. Cross-sectional transmission electron microscopy (XTEM) is a necessary tool of the investigation of irradiation-induced damage because it provides a direct measurement of the damage distribution and detailed microstructural information on the damaged zone, such as the presence of amorphous regions and the size, density, and chemical nature of defect aggregates. The purpose of this article is to report on the formation and growth of the amorphous layers due to 1.5 MeV Kr^+ irradiation in quartz at room temperature. We have characterized the accumulation of damage in quartz with increasing ion fluence using XTEM. The XTEM observations are compared to the TRIM calculations which provide the basis for the analysis of the results.

II. EXPERIMENT

Slices of ~200 μm thick were cut from a single crystal of α-quartz parallel to the (1010) plane. The slices were polished to a 50 μm in thickness using 9–30 μm diamond films. The polished slices were then drilled into 3-mm-diam disks. Only the side of a quartz disk, later polished by 0.05 μm colloidal silica, was irradiated by 1.5 MeV Kr^+ ions.

The irradiation was carried out at the HVEM-Tandem Facility at Argonne National Laboratory. This facility consists of a modified Kratos/AEI EM7 high-voltage electron microscope (HVEM) and a 2 MeV tandem ion accelerator.[15] The seven quartz disks for XTEM were irradiated with 1.5 MeV Kr^+ ions at room temperature, to the following fluences: 1.7×10^{12}, 8.5×10^{12}, 1.7×10^{13}, 3.4×10^{13}, 5.1×10^{13}, 8.5×10^{13}, and 1.7×10^{14}, ions/cm^2. Several prethinned transmission electron microscopy (TEM) samples were also irradiated with 1.5 MeV Kr^+ ions using the

a)Electronic mail: wgong@unm.edu

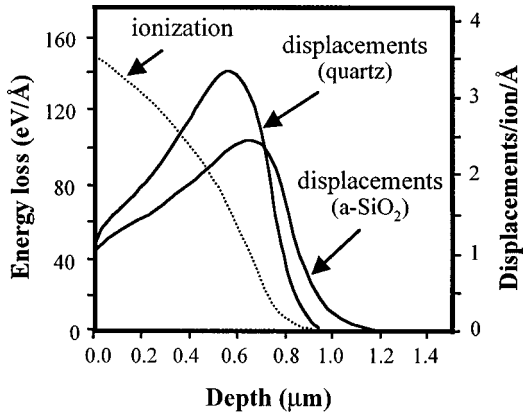

FIG. 1. Calculated distributions of energy loss displacement damage in α-quartz and amorphous silica, a-SiO_2, from 1.5 MeV Kr^+ irradiation based on TRIM-95.

HVEM-Tandem Facility with *in situ* TEM observations. The critical fluence for amorphization of quartz was 1.2×10^{14} ions/cm^2 for a maximum thickness ($\sim$300 nm) that can be penetrated by 300 keV electrons during *in situ* TEM.

The cross-sectional specimens were prepared using the so-called *T*-tool technique which is a modified tripod polishing technique.[16] The irradiated surface of the disk was first glued to a silicon wafer. The glued specimen was sectioned perpendicularly to the irradiation surface and was then polished down to the thickness at which the silicon wafer became transparent (for yellow–orange birefringence, the thickness is ~1 μm). The specimen was ion milled for surface cleaning and final thinning ($\sim$4 keV Ar^+ ions, 7°–9° sputtering angle). In this process, the silicon strip was used to monitor the sample thickness, as the color of the light transmitted through a silicon strip depends upon the silicon sample thickness as well as the type of light source.[17] Because of the minimal ion-milling time (20 min or less), artifacts arising from lengthy ion milling can be avoided. Most of the TEM analysis was performed using a JEM 2000FX microscope. High resolution transmission electron microscopy (HRTEM) analysis was performed using a JEM 2010 microscope with a Gatan® 694 slow scan charge coupled device camera. Both microscopes were operated at 200 keV.

The distribution of atomic displacements per ion and energy loss due to ionization are shown in Fig. 1 as functions of depth. The results were calculated using TRIM-95 (full cascades),[18] and a displacement energy of 10 eV for both Si and O in quartz.[11]

III. RESULTS AND DISCUSSION

XTEM micrographs (Fig. 2) show the early stages of damage accumulation in quartz. In all the micrographs, the specimen surface shown in the upper part of the picture is covered by the epoxy and the depth scale can be easily deduced.

A damage zone forms [Fig. 2(a)], after a fluence of 1.7×10^{12} ions/cm^2 ($\sim$0.01 dpa at the peak depth). The damage layer lies at a depth of 550–850 nm below the surface, corresponding to the peak displacement depth. The microdiffraction pattern of the damage layer reveals two diffuse

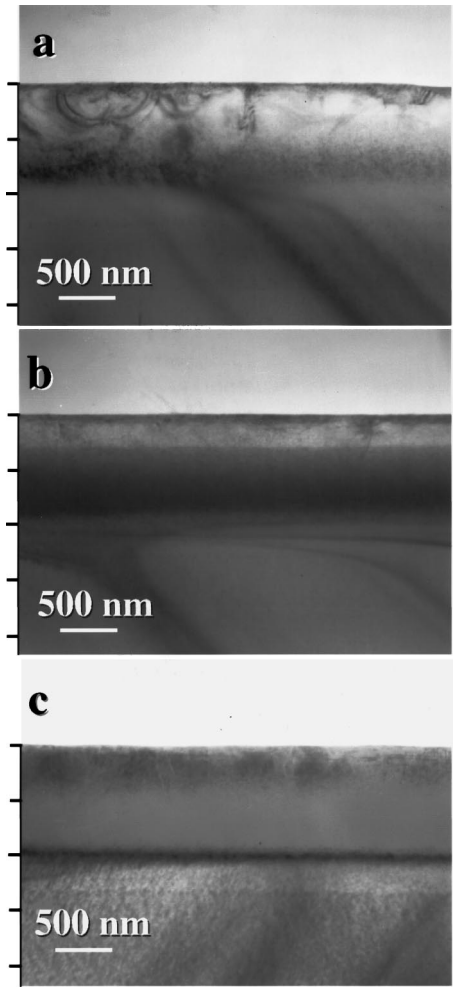

FIG. 2. XTEM micrographs showing the damage structure as a function of ion fluence at 300 K; (a) 1.7×10^{12} ions/cm^2, (b) 8.5×10^{12} ions/cm^2, and (c) 1.7×10^{13} ions/cm^2. The unit length of the vertical bar on the left is 500 nm.

rings, overlapping the sharp diffraction maxima, indicating the presence of amorphous volumes embedded in the still crystalline matrix. This is confirmed by the corresponding HRTEM image (Fig. 3). The image shows amorphous re-

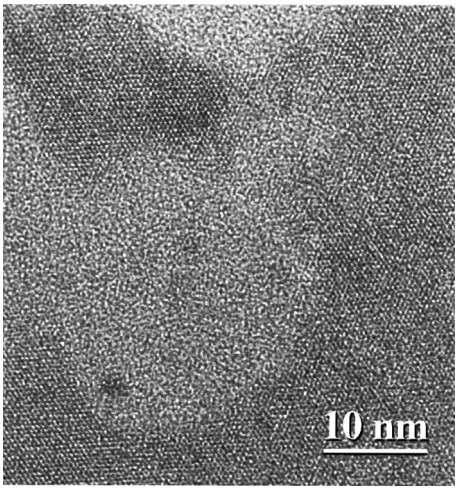

FIG. 3. HRTEM image from the damage layer at a depth of appropriately 700 nm after a fluence of 1.7×10^{12} ions/cm^2.

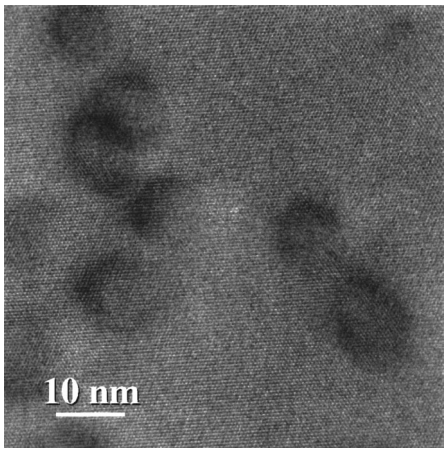

FIG. 4. HRTEM image of the upper portion of the cross section at a depth of 300 nm after a fluence of 1.7×10^{12} ions/cm^2. The strain center resemble those found in the electron-irradiated α quartz where ionization effects were dominant (see Refs. 10 and 19).

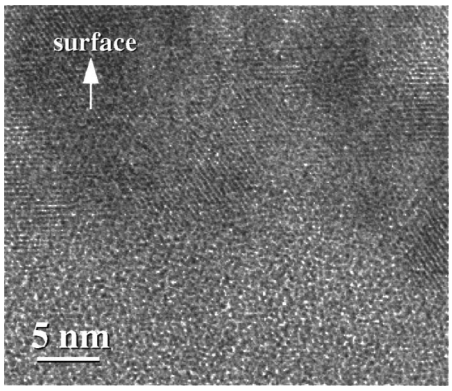

FIG. 5. HRTEM image of the amorphous-crystalline interface in the upper portion of the cross section after a fluence of 1.7×10^{13} ions/cm^2. Discontinuous lattice and twisted lattice fringes with mottled contrast suggest that the upper zone is not completely crystalline.

gions embedded in the crystalline matrix, suggesting that amorphization of Kr^+-irradiated quartz occurs through a heterogeneous displacement process instead of a homogeneous process, by which a gradual increase of point-defect concentration leads to a gradual change in image characteristic from that of a perfectly crystalline to an aperiodic material.[19] The homogeneous mechanism consists of a structural relaxation process of a highly damaged quartz matrix, triggered by a critical point defect concentration.[20] In contrast, the near-surface portion of the cross section, corresponding to the region with maximum electronic energy loss, is mostly crystalline as evidenced by both XTEM [Fig. 2(a)] and HRTEM images (Fig. 4). Individual strain centers appear in the crystalline matrix. This type of strain center has been reported in electron-irradiated quartz and coesite (a high-density polymorph of SiO_2) for which ionization is the dominant amorphization process.[21–23] The strain centers formed at the initial stage of electron irradiation can be nucleation sites for amorphous areas.[22] This indicates that the damage in the upper portion of the cross section is indeed dominated by ionization processes. As shown in Fig. 1, the dominant energy loss is by ionization at the near surface portion of the specimen. The collisional displacement profile for quartz (using density 2.65 g/cm^3) reaches its peak at a depth of 500–800 nm and ends at a depth of 950 nm. The damage profile observed by XTEM is in excellent agreement with that for the displacement damage predicted by TRIM calculations for quartz. XTEM results indicate that direct displacement by nuclear collision is more efficient in inducing amorphization in quartz than the ionization process.

At a fluence of 8.5×10^{12} ions/cm^2, a continuous amorphous layer has developed from the previously formed damage layer at a depth of 600–800 nm ($\sim$0.04 dpa at the peak displacement range), as shown by Fig. 2(b). After a fluence of 1.7×10^{13} ions/cm^2, the amorphous layer has grown toward the surface, and it spans across a depth range of 400–900 nm, with the presence of a crystalline-dominated zone on the near-surface portion of the specimen [Fig. 2(c)]. The displacements per atom is 0.07 for the peak displacement range (400–900 nm), while it is only 0.03 for the near-surface range (0–400 nm). The amorphous layer is homogeneous in image contrast, lacking of diffraction contrast from local bending, and is confirmed by the diffraction halo pattern and HRTEM imaging. The interface between the amorphous layer and the upper crystalline zone is not sharp (Fig. 5). Furthermore, the top zone is not perfectly crystalline. The lattice fringes are discontinuous or twisted and exhibit mottled contrast as shown by Fig. 5, which may be due to a high concentration of point defects or the presence of small amorphous volumes. As compared with Fig. 4 taken at a lower fluence, the lattice fringes show ''fuzzy'' contrast in the matrix. This suggests that amorphization may also proceed in slower homogeneous manner when ionization dominates the near-surface region.

The present XTEM results are consistent with the RBS-C measurements on ion-beam-induced amorphization of quartz by Harbsmeier and Boise.[24] There is a critical fluence at which a buried amorphous layer formed. At higher fluences, the continuous amorphous layer grows toward the surface and into larger depths.

Figure 6 presents a set of XTEM micrographs showing that amorphization proceeds toward both the top surface and the interior regions of the quartz crystal under continued irradiation at room temperature. After a fluence of 3.4×10^{13} ions/cm^2, the amorphization front is at a depth of $\sim$950 nm, and the upper crystalline portion of the specimen that was observed at a lower fluence (e.g., 1.7×10^{13} ions/cm^2), has been fully amorphized [Fig. 6(a)]. The fluence is 0.06 dpa at the near-surface region and 0.14 dpa at the peak displacement depth. For comparison, the prethinned TEM sample was amorphized at a relatively higher fluence ($\sim1.2\times10^{14}$ ions/cm^2) as indicated by *in situ* TEM. However, the XTEM results indicate that a surface layer $\sim$950 nm in thickness is fully amorphized at a relatively low fluence (3.4×10^{13} ions/cm^2). During the *in situ* experiments using the HVEM-Tandem Facility, a 1.5 MeV Kr^+ ion beam was used to irradiate the specimen, and a 300 keV electron beam was used for the *in situ* TEM observations. Thus, the effect of concurrent irradiation with electrons on ion-ionization-induced amorphization should be considered. The concurrent effect

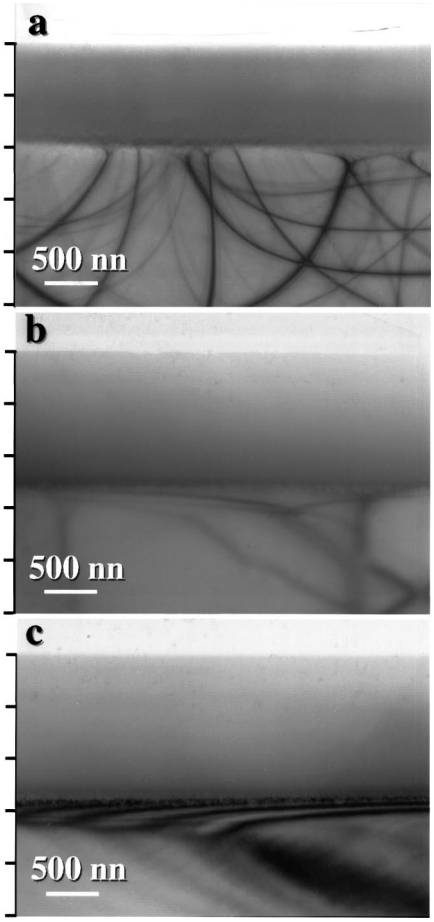

FIG. 6. XTEM micrographs showing continuous growth of the amorphous layer with increasing ion fluence at 300 K; (a) 3.4×10^{13} ions/cm^2, (b) 8.5×10^{13} ions/cm^2, and (c) 1.7×10^{14} ions/cm^2. The unit length of the vertical bar on the left is 500 nm.

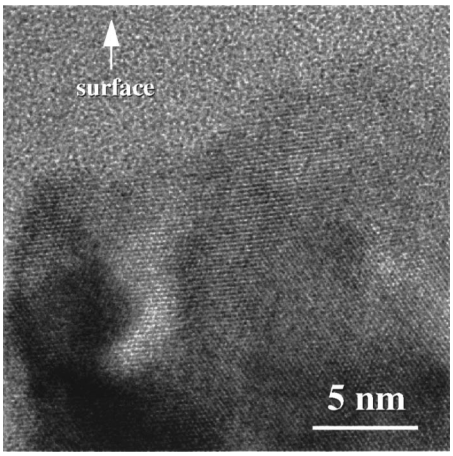

FIG. 7. HRTEM image of the amorphous–crystalline interface within the bottom portion of the cross section after a fluence of 1.7×10^{14} ions/cm^2. The irradiation-induced strain field is evident in the region close to the interface as indicated by the dark contrast.

of electron irradiation on ion-induced amorphization has been observed to retard ion-induced amorphization in Si crystals.[25] Electrons of low energy may retard the process of ion-induced amorphization through ionization-enhanced point defect diffusion and recombination.[26,27] Also, a free surface may act as a sink for point defects. Therefore, a higher critical fluence for ion-induced amorphization of the thin foil specimen is to be expected.

With the ion fluence increased to 5.1×10^{13} ions/cm^2, the amorphization front has moved to a depth of ~1100 nm below the surface. After a fluence of 8.5×10^{13} ions/cm^2, the amorphization front is at a depth of ~1250 nm [Fig. 6(b)]. With a fluence up to 1.7×10^{14} ions/cm^2, the amorphization front had extended to a depth of nearly 1400 nm [Fig. 6(c)]. Data in Fig. 6 indicate that with increasing ion fluence, the amorphous layer may extend into the deeper regions of the quartz crystal, far beyond the damage range predicted by the TRIM calculations (Fig. 1). The range ratio of the theoretical an the XTEM measured values, $R_{\mathrm{XTEM}}/R_{\mathrm{TRIM}}$ is close to 1 for the quartz irradiated at lower ion fluences ($\leqslant1.7\times10^{13}$ ions/cm^2). In this case, the upper portion of the cross section for the quartz crystal is not fully amorphized. However, for high ion fluences (e.g., 1.7×10^{14} ions/cm^2) $R_{\mathrm{XTEM}}/R_{\mathrm{TRIM}}$ increases to ~1.5. Arnold has completed systematic range measurements for 250 keV ions at 1×10^{16} ions/cm^2 on quartz using optical microscopy and Rutherford backscattering.[28] Arnold found that there is a threshold value for collisional energy deposition at which the effective or extended damage depth begins to markedly exceed the TRIM values. As the XTEM results shows [Fig. 6(a)], complete amorphization is reached within the TRIM calculated range, 950 nm, at a fluence $\leqslant3.4\times10^{13}$ ions/cm^2. The change in density of quartz, from 2.65 g/cm^3 for α-quartz to about 2.25 g/cm^3 for amorphous silica (a-SiO_2), is caused by amorphization. The damage profile was then recalculated using TRIM-95 assuming a density of 2.25 g/cm^3 for a-SiO_2 with an ion fluence $\geqslant3.4\times10^{13}$ ions/cm^2. A shown in Fig. 1, the calculated damage range now shifts to a depth of ~1200 nm. However, our XTEM results indicate that the amorphization depth still exceeds the TRIM predicted value in a-SiO_2. The discrepancy in the damage range between the XTEM and TRIM results may be explained by the effect of irradiation-induced stress as suggested for ion-irradiated glasses by Arnold *et al.*[29] Large strain fields may be produced at the crystalline–amorphous ($c-a$) interface due to the volume expansion in the amorphous material. The dark contrast indicate that a large gradient of stress exists in the deeper crystalline region close to the interface (Fig. 7). Plastic or viscous flow can be produced during ion-irradiation-induced amorphization.[30–33] Some part of energy may be transported beyond the end-of-range along the stress gradient through point defect diffusion. Thus, ion implantation in glasses including amorphous silica, produces structural modifications at depths greater than those of the implanted ion range.[29] The existing $c-a$ interface may play an important role in causing the extension of the amorphous layer into the undamaged, underlying region of the crystal. Pre-existing $c-a$ interfaces can act as nucleation sites for amorphization leading to amorphous layer growth in Si (Ref. 34) and coesite.[35]

The discrepancy in the damage range between the XTEM and TRIM results may be also explained by the dimensional change caused by the irradiation. The relative dimensional change has been reported to be ~10% for quartz

during 340 keV Xe^+ irradiation ($\sim 10^{14}$ Xe^+/cm^2) at 458 K.[31] Mechanical surface profiling has revealed that large compressive stresses ($\sim$1.5 GPa) build up at the low fluences for which the amorphous layer has not extended to the surface.[24] The stresses are released at higher fluences after the amorphous layer extends to the surface. The stress release is accompanied by a significant reduction of the atomic density by $\sim$19%.[24] The surface profile measurement of quartz irradiated with 50 keV Na^+ at a fluence of 1×10^{15} ions/cm^2 showed that the volume swelling occurred vertically.[24] In the case of 1.5 MeV Kr^+-induced amorphization of quartz, the damage range predicted by TRIM is $\sim$1200 nm. Assuming 10% dimensional change, then the damage range is expected to be $\sim$1320 nm which is close to the XTEM measured value for a fluence of 1.7×10^{14} ions/cm^2, $\sim$1400 nm. In contrast, large compressive stresses build up at lower fluences ($<3.4\times10^{13}$ ions/cm^2), and the dimensional change is insignificant when the amorphous layer has not extended to the surface. Thus, the damage range predicted by TRIM is consistent with the XTEM measured value.

IV. CONCLUSIONS

XTEM and HRTEM have been successfully used to study the damage formation and growth of amorphous layers in α-quartz by 1.5 MeV Kr^+ irradiation at room temperature.

(1) A damage layer is first induced at a depth of 550–850 nm corresponding to the peak depth of the displacement damage. The amorphous regions embedded in the damage layer are formed through a displacement damage process. In contrast, ionization dominates the near-surface region. With increasing ion fluence, a continuous amorphous layer developed from the previously formed damage layer, and this region grows toward the sample surface until the top zone becomes completely amorphous at a fluence of 3.4×10^{13} ions/cm^2.

(2) The damage profile observed by XTEM is in excellent agreement with that of damage predicted by TRIM calculations at a fluence $<3.4\times10^{13}$ ions/cm^2 at which the amorphus layer has not extended to the surface. Direct displacement by nuclear collision is more efficient in inducing amorphization than the ionization process.

(3) With increasing ion fluences, up to 1.7×10^{14} ions/cm^2, the amorphous layer measured by XTEM extends steadily deeper into the quartz crystal until reaching a depth of $\sim$1400 nm. This exceeds the TRIM predicted value, $\sim$1200 nm in a-SiO_2 (with a density of 2.25 g/cm^3). If 10% of the dimensional change caused by the relaxation process of the compressed amorphous phase is considered, then the damage range is expected to be 1320 nm, close to the XTEM measured value ($\sim$1400 nm).

ACKNOWLEDGMENTS

The authors thank the HVEM-Tandem Facility staff at Argonne National Laboratory for assistance during ion beam irradiations and Dr. L. F. Chen for assistance during sample preparation and TEM observations. The electron microscopy was completed in the Microbeam Analysis Facility of the Department of Earth and Planetary Sciences at the University of New Mexico. This study has been supported by the office of Basic Energy Sciences and the Environment Management Sciences Program, U.S. Department of Energy under Contract No. DE-FG02-97ER45656.

[1] G. H. Beall, in *Silica: Physical Behavior, Geochemistry, and Materials Applications*, edited by P. J. Heaney, C. T. Prewitt, and G. V. Gibbs (Mineralogical Society of America, Washington, D.C., 1994).
[2] C. R. Helms and B. E. Deal, *The Physics and Chemistry of SiO_2 and Si-SiO_2 Interface 2* (Plenum, New York, 1993).
[3] P. D. Townsend, P. J. Chandler, and L. Zhang, *Optical Effects of Ion Implantation* (Cambridge University Press, Cambridge, 1994).
[4] P. Martin, M. Dufour, A. Ermolieff, S. Marthon, F. Pierre, and M. Dupov, J. Appl. Phys. **72**, 2907 (1992).
[5] P. D. Townsend, Nucl. Instrum. Methods Phys. Res. B **65**, 243 (1992).
[6] K. Wenzlik, J. Heibei, and E. Voges, Phys. Status Solidi A **61**, K207 (1980).
[7] P. J. Chandler, L. Zhang, and P. D. Townsend, Nucl. Instrum. Methods Phys. Res. B **46**, 69 (1990).
[8] N. D. Skelland and P. D. Townsend, J. Phys. D **27**, 1672 (1994).
[9] C. B. Norris and E. P. EerNisse, J. Appl. Phys. **45**, 3876 (1974).
[10] L. W. Hobbs and M. R. Pascucci, J. Phys. C **41**, 237 (1980).
[11] R. L. Pfeffer, J. Appl. Phys. **57**, 5176 (1985).
[12] H. Fischer, G. Gotz, and H. Karge, Phys. Status Solidi A **76**, 249 (1983).
[13] R. G. Macaulay-Newcombe, D. A. Thompson, J. A. David, and D. V. Stevanovic, Nucl. Instrum. Methods Phys. Res. B **46**, 180 (1990).
[14] L. M. Wang, Nucl. Instr. Meth. Phys. Res. (in press).
[15] C. W. Allen, L. L. Funk, E. A. Ryan, and A. Taylor, Nucl. Instrum. Methods Phys. Res. B **40/41**, 553 (1989).
[16] R. Anderson, S. J. Klepeis, J. P. Benedict, W. G. Vandygrift, and M. Orndorff, Inst. Phys. Conf. Ser. **100**, 491 (1989).
[17] J. P. McCaffrey, B. T. Sullivan, J. W. Fraser, and D. L. Callahan, Micron **27**, 407 (1996).
[18] J. F. Ziegler, J. P. Biersack, and U. Littmark, *The Stopping and Range of Ions in Solids* (Pergamon, New York, 1985).
[19] J. Washburn, C. S. Murty, D. Sadana, P. Byrne, R. Gronsky, N. Cheung, and R. Kilaas, Nucl. Instrum. Methods Phys. Res. **209/210**, 345 (1983).
[20] L. Douillard and J. P. Duraud, Nucl. Instrum. Methods Phys. Res. B **107**, 212 (1996).
[21] M. R. Pascucci, J. L. Hutchison, and L. W. Hobbs, Radiat. Eff. **74**, 219 (1983).
[22] H. Inui, H. Mori, T. Sakata, and H. Fujita, J. Non-Cryst. Solids **116**, 1 (1990).
[23] W. L. Gong, L. M. Wang, R. C. Ewing, and J. Zhang, Phys. Rev. B **54**, 3800 (1996).
[24] F. Harbsmeier and W. Boise, J. Appl. Phys. **83**, 4049 (1998).
[25] H. Abe, C. Kinoshita, P. R. Okamoto, and L. E. Rehn, J. Nucl. Mater. **212–215**, 298 (1994).
[26] J. Koike, P. R. Okamot, L. E. Rehn, and M. Meshii, Metall. Trans. A **21**, 1799 (1990).
[27] S. J. Zinkle, J. Nucl. Mater. **219**, 113 (1995).
[28] G. W. Arnold, Nucl. Instrum. Methods Phys. Res. B **65**, 213 (1992).
[29] G. W. Arnold, G. Battaglin, A. Boscolo-Boscoletto, F. Cacavale, G. De Marchi, P. Mazzodli, and A. Miotello, Nucl. Instrum. Methods Phys. Res. B **65**, 387 (1992).
[30] C. A. Volkert, J. Appl. Phys. **70**, 3521 (1991).
[31] A. Benyagoub, S. Loffler, M. Rammensee, and S. Klaumunzer, Nucl. Instrum. Methods Phys. Res. B **65**, 228 (1992).
[32] E. Snoeks, T. Weber, A. Cacciato, and A. Polman, J. Appl. Phys. **78**, 4723 (1995).
[33] M. L. Brongersma, E. Snoeks, and A. Polman, Appl. Phys. Lett. **71**, 1628 (1997).
[34] H. A. Atwater and J. S. Im, Nucl. Instrum. Methods Phys. Res. B **59/60**, 386 (1991).
[35] W. L. Gong, L. M. Wang, R. C. Ewing, and H. S. Xie, J. Appl. Phys. **81**, 2570 (1997).